Internal signal correlates neural populations and biases perceptual decision reports

Federico Carnevale[a], Victor de Lafuente[b], Ranulfo Romo[c,d,1], and Néstor Parga[a,1]

[a]Departamento de Física Teórica, Universidad Autónoma de Madrid, Cantoblanco 28049, Madrid, Spain; [b]Instituto de Neurobiología, Universidad Nacional Autónoma de México, 76230 Querétaro, Mexico; [c]El Colegio Nacional, 06020 Mexico D.F., Mexico; and [d]Instituto de Fisiología Celular-Neurociencias, Universidad Nacional Autónoma de México, 04510 Mexico D.F., Mexico

Contributed by Ranulfo Romo, September 29, 2012 (sent for review July 17, 2012)

In perceptual decision-making tasks the activity of neurons in frontal and posterior parietal cortices covaries more with perceptual reports than with the physical properties of stimuli. This relationship is revealed when subjects have to make behavioral choices about weak or uncertain stimuli. If knowledge about stimulus onset time is available, decision making can be based on accumulation of sensory evidence. However, the time of stimulus onset or even its very presence is often ambiguous. By analyzing firing rates and correlated variability of frontal lobe neurons while monkeys perform a vibrotactile detection task, we show that behavioral outcomes are crucially affected by the state of cortical networks before stimulus onset times. The results suggest that sensory detection is partly due to a purely internal signal whereas the stimulus, if finally applied, adds a contribution to this initial processing later on. The probability to detect or miss the stimulus can thus be explained as the combined effect of this variable internal signal and the sensory evidence.

pairwise correlations | perception | somatosensory | cortex

Animals often make perceptual decisions under uncertain conditions (1–14). The arrival of a behaviorally relevant sensory stimulus is usually unknown and its presence is often ambiguous because it can be weak and appear in a noisy background. What are the neural mechanisms underlying the decision-making process in this situation? Neurophysiological experiments often use clear cues indicating when to start gathering the sensory evidence on which decisions are based (2, 13). In these paradigms, experimental data can be explained by feed-forward accumulation models (1, 2, 5, 14). However, when the time of stimulus onset is variable, neural integration of sensory signals is problematic because it would start either too soon, in which case noise will dominate the process, or too late, losing part of the signal. There is evidence that the brain uses internal signals to guide detection of sensory stimuli (15). These signals are related to task contingencies that prefrontal cortical networks acquire during training (16) and combine with the stimulus to produce the behavioral response following a process different from simple integration of the sensory evidence (13).

To further investigate the neuronal mechanisms coping with uncertainty about stimulus onset and the role of internal signals in sensory perception, we recorded the simultaneous activity of pairs of premotor cortex neurons, while trained monkeys performed a vibrotactile detection task (11, 12). In this task, the stimulus was often absent or weak, and the time of its application varied uniformly within a 2-s time interval (Fig. 1*A* and *Materials and Methods*). Previously, it was found that the activity of single neurons covaries with the subject's decision report. Here, by analyzing pairwise spike-count correlations, we take a population-level approach. This allows us to uncover a purely internal signal that affects the population of neurons and increases the correlation between them.

Results

Premotor Cortex Activity Is Modulated During the Task. The temporal profiles of neuronal firing rates covary with the decision report (11, 12) (Fig. 1*B*). Interestingly, the firing rate activity during false-alarm trials is higher than during miss and correct-reject trials. This could be an indication that premotor cortex neurons are receiving a stimulus-independent signal. If an internal signal were collectively affecting the neural population, the firing rate of pairs of neurons would cofluctuate, perhaps in a time-dependent manner. We have then analyzed the time course of the spike-count correlations of pairs of simultaneously recorded premotor cortex neurons (11, 12). We start by noting that these noise correlations are modulated during the course of a trial. The temporal profile of the spike-count correlation coefficient (CC), defined in a time window of 250 ms and computed using stimulus-present trials (hits and misses) aligned at the stimulus onset, is shown in Fig. 1*C*. Before stimulus presentation, CCs are relatively weak. Following stimulus onset, and with latency similar to firing rate responses (12), CCs grow until they are more than twice their initial value.

When trials are segregated according to the animal's decision reports, the time course of the CCs appears modulated in a condition-dependent manner (Fig. 1*D*). One notes that (*i*) the CCs in miss and correct-reject trials have similar temporal profiles, except during the stimulus period and the subsequent relaxation in miss trials; (*ii*) in hit trials they reach higher values during the stimulation period; (*iii*) the CCs in false-alarm trials are higher than in correct-reject trials during the first half of the shown interval; and (*iv*) noise correlations can be weak; their smallest values, in the four conditions, are attained during the last portion of the delay period, reaching mean values of about 0.06, in agreement with measurements in the supplementary motor area during simple reaching tasks (17). This is seen in Fig. 1*D*, *Inset*, showing the distribution of CCs in correct-reject trials at the end of the delay period. Previous recordings in prefrontal cortex of monkeys performing a working memory task studied the time course of CCs, but correlations were not modulated at any task stage (18).

Spike-Count Correlations and Firing Rate Activity Reveal a Purely Internal Processing. A closer view of Fig. 1*D* shows that before stimulus onset the CCs in hit trials are higher than those obtained for correct rejection trials at any time. This could be another manifestation of an internal signal that, starting before stimulus onset, modulates the activity of premotor cortex neurons and might influence the outcome of the decision-making process. To further explore the properties of this signal, we computed the CCs by aligning the trials when monkeys place their nonstimulated hand on the immovable key [key down (KD)] (Fig. 1*A*). This event is important because it initiates the 1.5- to 3.5-s variable period that precedes stimulus onset. We hypothesized

Author contributions: R.R. and N.P. designed research; V.d.L. and R.R. performed research; F.C. and N.P. analyzed data; and F.C., V.d.L., R.R., and N.P. wrote the paper.

The authors declare no conflict of interest.

[1]To whom correspondence may be addressed. E-mail: rromo@ifc.unam.mx or nestor.parga@uam.es.

This article contains supporting information online at www.pnas.org/lookup/suppl/doi:10.1073/pnas.1216799109/-/DCSupplemental.

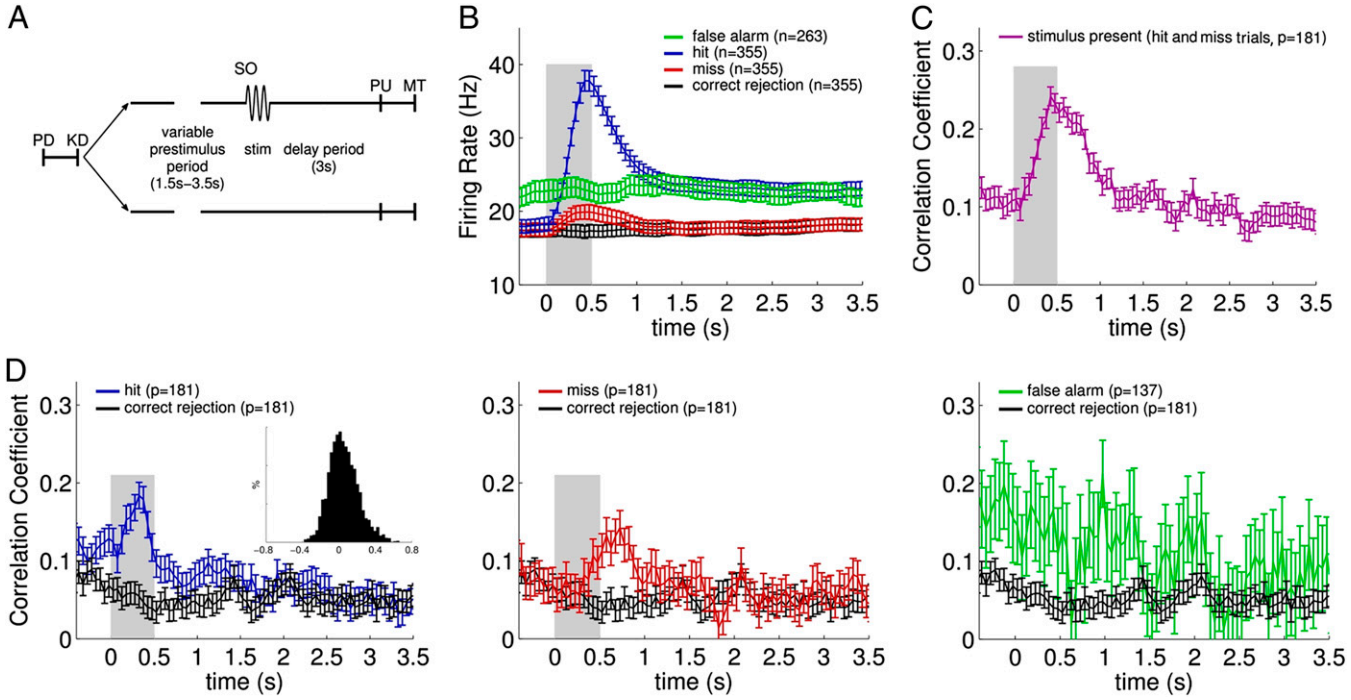

Fig. 1. Detection task and temporal profile of firing rates and spike-count correlation coefficients. (*A*) The mechanical probe was lowered, indenting the skin of one fingertip of the restrained hand (PD) and the monkey reacted, placing its free hand on an immovable key (KD). After a variable prestimulus period from 1.5 to 3.5 s, on half of the trials a vibratory stimulus of 0.5 s duration was presented (SO). After a fixed delay period of 3 s the stimulator probe moved up (PU), indicating to the monkey that it could make the response movement (MT) to one of the two buttons. The button pressed indicated whether or not the monkey felt the stimulus. (*B*) Temporal profile of the firing rates according to the behavioral conditions (*n*, number of neurons). Stimulus-present trials were aligned at SO and stimulus-absent trials were aligned at PU. The gray box marks the time of stimulus presentation. (*C*) Temporal profile of correlation coefficients (CCs) of spike counts using stimulus-present trials (hits and misses) aligned at the SO (*p*, number of pairs). The gray box marks the time of stimulus presentation. (*D*) Temporal profile of CCs according to behavioral conditions. Stimulus-present trials (hits and misses) were aligned at SO and stimulus-absent trials (false alarms and correct rejections) were aligned at PU. The time courses of the CCs are modulated in a condition-dependent manner. Bars indicate confidence intervals, 90% significance level, two sided (*Materials and Methods*). *Inset* shows the CCs population histogram of neuron pairs from $t = 2$ to $t = 3$ s from SO for correct-reject trials.

that if premotor cortex neurons reflect the animal's use of the knowledge of stimulus onset times, modulation of their CCs should start roughly at 1.5 s. Again, the time course of the CCs depends on the behavioral condition (Fig. 2*A*). In stimulus-present trials, we computed the time course of these coefficients, keeping trials only until the application of the stimulus. In all decision reports, we observed a modulation that seems to be driven by the internal signal. The temporal profiles of CCs during miss and correct-reject trials are similar (Fig. 2*A*). In accordance with the hypothesis that the internal signal influences the decision reports, we observed that during hit and false-alarm trials the CCs undergo a large positive fluctuation beginning about 1.5 s after KD. Similar temporal dynamics can be observed in the firing rates: Whereas in correct-reject and miss trials they become stationary soon after KD, in false-alarm and hit trials they begin to increase at about 1.5 s (Fig. 2*B*).

The modulated activity occurring before stimulus onset is consistent with the hypothesis that premotor cortex neurons make use of task contingencies to prepare the network for the stimulus arrival. The higher average firing rate in false-alarm trials beginning from KD suggests the presence of an internal signal controlling the excitability of the neurons that fluctuates from trial to trial. Its effect in the other behavioral conditions is less evident presumably because it is weak and therefore the probability that neurons reach their firing-rate threshold is low (Fig. 2*B*). However, the fluctuating nature of the signal can be made more visible in the hit condition by restricting the computation of firing rates to trials with weak stimulus amplitudes (less than 6 μm) and mean firing rates higher than 6 Hz (Fig. 2*C*). The internal signal has an appreciable strength as can be seen by comparing the change in firing rate that occurs in false-alarm trials at 1.5 s after KD (about 5 Hz) with the changes produced by the stimulus in hit trials (about 20 Hz) and in miss trials (about 3 Hz).

Activity of Premotor Cortex Neurons Covaries at Slow Temporal Scales. The presence of temporally modulated noise correlations before stimulus onset suggests that the fluctuating signal is common to a substantial number of neurons. To quantify this effect we studied the covariation of pairs of neurons at scales longer than $T = 500$ ms. Slow excitability cofluctuations of specific pairs can be detected by comparing the covariance of the spike counts of the neurons, defined in a time window of size T, with the product of the two spike counts. Because the spike-count variable does not have information about fluctuations at scales shorter than T, the remaining covariations are guaranteed to originate from slower scales. On the other hand, the product of the spike counts supports the hypothesis of firing independence at scales longer than T. If two neurons did not cofluctuate at long timescales, these two quantities should be equal; a nonzero value of their difference E reveals the presence of slow covariations (*Materials and Methods*). This analysis confirms that premotor cortex neurons do covary at timescales longer than 500 ms. To trace the effect of the internal signal on the population of pairs, we computed the distribution of E at two different 500-ms bins of the task during hit trials (before stimulus onset and at the end of the delay period). The result in Fig. 3*A*, *Left* indicates that before stimulus onset many pairs share the internal signal, but by the

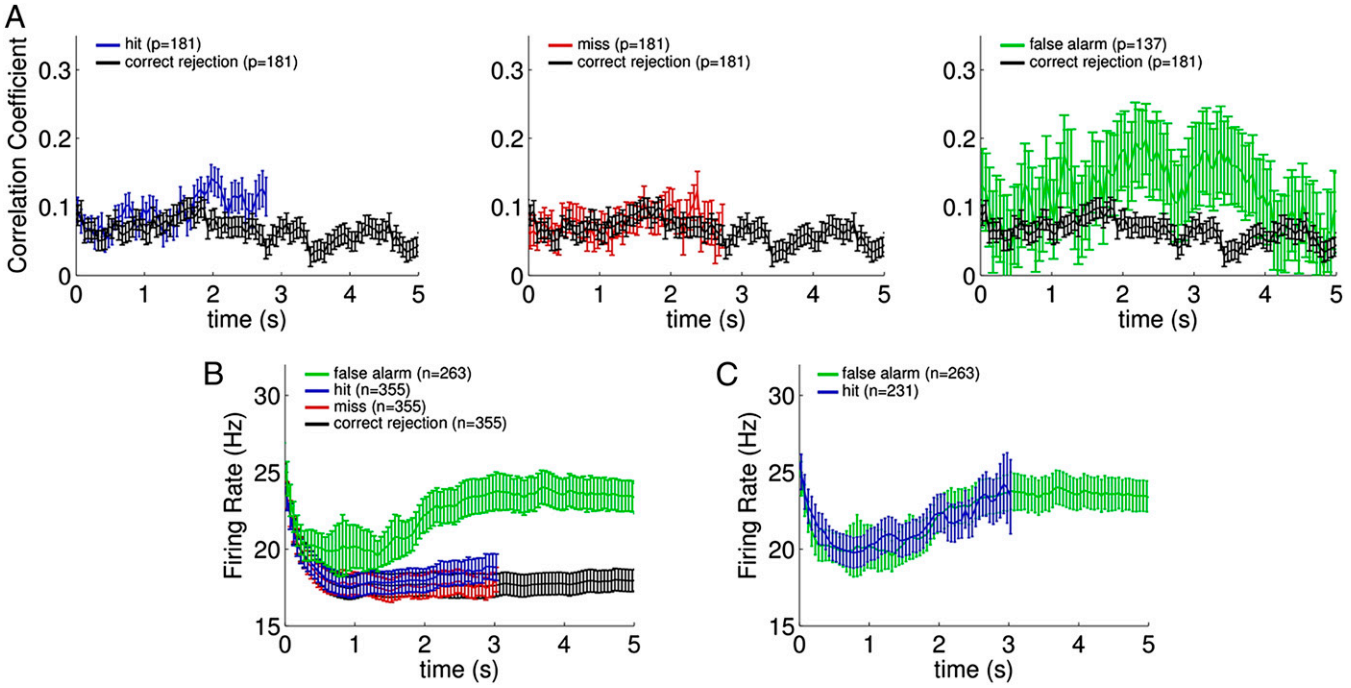

Fig. 2. Temporal profile of the spike-count correlation coefficients and mean firing rates in trials aligned at key down (KD). Trials were segregated according to behavioral condition and stimulus-present trials were kept only until stimulus onset. (*A*) Time course of CCs for each behavioral condition (*p*, number of pairs). During hit and false-alarm trials the CCs increase starting ~1.5 s after KD. Bars indicate confidence intervals, 90% significance level, two sided (*Materials and Methods*). (*B*) Mean firing rate in each behavioral condition (*n*, number of neurons). As with the CCs, in hit and false-alarm trials, the firing rate increases after 1.5 s immediately after KD. (*C*) Mean firing rate of a subset of hit trials equivalent to the mean firing rate of false alarms. This subset was obtained by selecting those hit trials with weak amplitudes (less than 6 μm) that had mean firing rate higher than 6 Hz.

end of the delay period the fraction of pairs with a low level of covariation increases substantially (Fig. 3*A*, *Right*). The long tail exhibited by the distribution in the prestimulus period disappears during the delay period, being replaced by a larger peak at the origin (Fig. 3*B*).

Statistical Model Predicts Performance and Correlation Coefficients. The results presented in Figs. 2 and 3 demonstrated that the processing taking place before stimulus onset significantly affected the behavioral response. To further analyze the role of the internal signal in the decision-making process, we implemented a statistical model of the cortical network activity during stimulus presentation. In the model, the membrane potential V_i of each neuron i results from the contribution of three components: $V_i = V_{0i} + V_s + V_{\text{int}}$. The first term represents the membrane potential of neuron i in the absence of any input besides noise. These are random variables that, for the sake of simplicity, we have drawn from a multivariate Gaussian distribution with homogeneous variance (σ_v) and membrane correlation coefficient (ρ). The second component, V_s, represents the membrane depolarization evoked by the stimulus and is obtained from the mean firing rates of primary somatosensory cortex (S1) neurons (11). The last component, V_{int}, denotes a trial-to-trial fluctuating common signal that we generated from an exponential distribution with mean μ_{int}. The firing rate is obtained from the membrane potential V_i with a sigmoidal activation function. The animal's decision is modeled using a decision rule based on the comparison of the population firing rate with a threshold (see *SI Text 1–3* for further details).

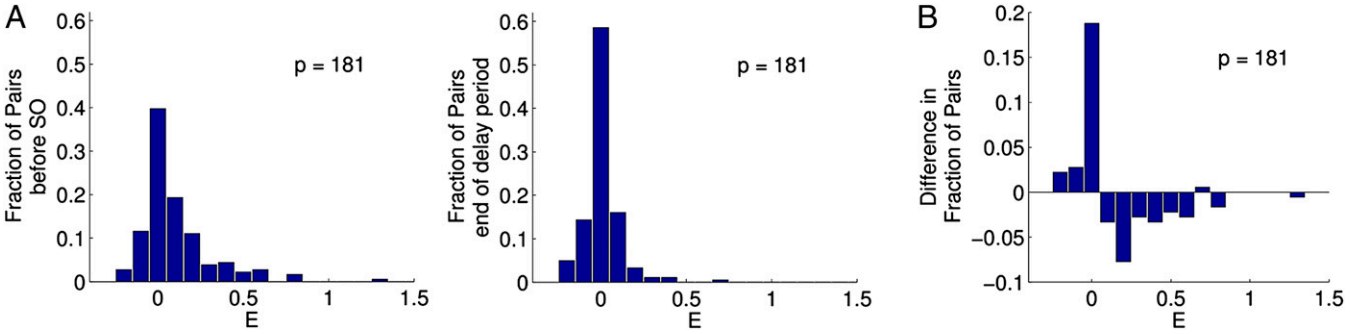

Fig. 3. Analysis of slow covariations. (*A*) Distribution of *E* (*Materials and Methods*) for 181 pairs of neurons before SO (*Left*) and at the end of the delay period (*Right*). Mean value of $E = 0.10$ during the prestimulus period, but reduces to 0.01 at the end of the delay period. (*B*) Difference in the fraction of pairs between the prestimulus period and the end of the delay period. Many pairs share the internal signal before the application of the stimulus, but little before the animal reports; the fraction of pairs with a low level of covariation increases substantially.

In the absence of stimulation, low values of the internal signal produce correct rejections whereas high values lead to false alarms (Fig. 4*A*, *Upper*). In stimulus-present trials low values of V_{int} produce misses whereas high values lead to hits (Fig. 4*A*, *Lower*). Because of the depolarizing effect of the stimulus, the boundary value of V_{int} that separates yes from no responses in stimulus-present trials is smaller than in stimulus-absent trials (Fig. 4*A*). Errors can be explained in terms of the common signal. The predicted frequencies of miss and false-alarm reports are in full agreement with the observed values (Fig. 4*B*). More generally, the predicted psychometric curve matches well the psychophysical reports (Fig. 4*C*) (11, 12).

Our experimental findings and our simulations suggest that the behavioral response results from the combination of the internal signal and the stimulus amplitude. The mean depolarization induced by the internal signal in each condition can be computed using the model (Fig. 4*D*). In stimulus-absent trials, large enough values of this signal produce false-alarm responses. In stimulus-present trials these large values give rise to hits; however, correct responses can be also obtained with weaker internal signals because of the extra depolarization produced by the stimulus. Correct rejections require low signal values and misses are produced with even weaker signals. The model can also be used to analyze the origin of the observed noise correlations for each behavioral condition. Possible sources of correlations are (*i*) membrane potential correlations, ρ, representing the effect of common recurrent inputs and spike correlations in the network; (*ii*) slowly varying excitability covariations, generated by the common internal signal; and (*iii*) effects from the sensory input. Interestingly, the model reproduces the observed CCs without correlating explicitly the potentials of the neurons, that is, taking $\rho = 0$ (Fig. 4*E*). This would mean that noise correlations have to come from other sources (19, 20). In stimulus-absent trials the only possible source is the internal signal; its larger value in false alarms compared with correct rejections (Fig. 4*D*) produces larger CCs in the first of these conditions. A similar argument explains that the CCs are higher in hit than in miss trials. Stimulation contributes positively to noise correlations; this explains why the CCs in misses are larger than in correct rejections even when the internal signal is larger for the second condition.

Discussion

The neuronal fluctuations described above occurring before stimulus onset could be reflecting the initiation of the decision-making process. If so, some features of the strategy developed by animals to solve the detection task can be inferred from the neuronal activity preceding stimulus onset. If this is the case, the problem posed by the uncertainty in the task could be solved by applying an internal reference signal at that time. If the strength of this pulse were such that in the absence of stimulation the population activity remained below the decision criterion and if the weakest stimulus were large enough to put it just above it, in principle the task could be performed well. However, noise spoils this strategy. A possible way to deal with this situation is to take into account the history of the decision reports during previous trials to modify in a flexible way the behavioral response in the current trial, something that could be implemented by modulating the neuronal depolarization at long timescales. In this context, the activity during the prestimulus period would be related to the inference about the presence of the stimulus in the current trial on the basis of the recent history. In fact, in this task, the number of yes responses before false-alarm trials is larger than in the set of all trials (8), which is an indication that the decision-making process uses memory in a timescale longer than one trial.

The internal fluctuating signal could be produced by neuromodulatory systems, which are known to be involved in decision-making tasks (21–25). In the task studied here, the activity of midbrain dopamine neurons is correlated with the monkey's decision report (22, 23). However, it does not present important modulations during the prestimulus period. The noradrenergic system has been suggested to be related to uncertainty aspects in detection tasks (24, 25), but experimental studies concluded that this signal is produced after the decision has been made in cortical areas (24). Thus, it is unlikely that this system could play a role in the activity changes observed during the prestimulus period.

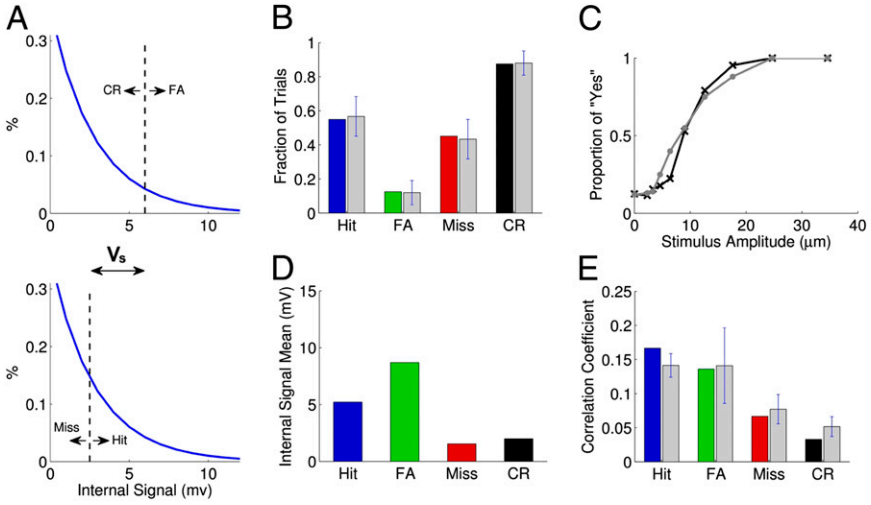

Fig. 4. Statistical model predicts the psychometric curve and the CCs. (*A*) Exponential distribution over trials of the fluctuating internal signal. In the absence of stimulation (*Upper*), low values of the internal signal produce correct rejections whereas high values lead to false alarms. In stimulus-present trials (*Lower*), low values of the internal signal produce misses whereas high values lead to hits. Because of the depolarizing effect of the stimulus, the value of the internal signal that separates "yes" from "no" responses in stimulus-present trials is smaller than that in stimulus-absent trials (dashed vertical lines). (*B*) Predicted mean fraction of trials for each behavioral condition (colored bars) compared with the experimental values (gray bars). (*C*) Model prediction of the psychometric curve (black crosses) compared with the experimental psychometric curve (gray circles). (*D*) Mean value of the internal signal averaged over the population and over trials of each behavioral condition. (*E*) Predicted mean CCs averaged over all pairs and over trials for each behavioral condition (colored bars). Gray bars represent experimental values. Results in *A*–*E* have been obtained assuming negligible voltage correlations ($\rho = 0$).

Although the current evidence seems to be against noradrenaline being responsible for the generation of the fluctuating signal, this conclusion has to be taken with some caution because a task with the same type of uncertainty present in our work has not been studied experimentally.

The activity observed during the prestimulus period may result from reverberating activity occurring in a distributed set of prefrontal and premotor areas that have been shown to be involved in working memory (3, 8, 10, 13, 26), decision making (8, 10, 13, 27), stimulus selection, and movement preparation (28–30).

Accumulator models (1, 2, 5, 14) have been successful in explaining some decision-making experiments (5, 14). However, as noted previously in sensory areas (15), feed-forward bottom-up processing cannot fully explain the experimental results. In our detection task, the time when accumulation of sensory evidence should start is ambiguous, but the moment after which the stimulus could be applied is well defined and the neural population does initiate integration at that time (Fig. 2 *B* and *C*). However, this integration is effective only if cells are sufficiently depolarized. Thus, the behavioral response could be the result of a combination of the internal signals and the sensory input; hit responses may result from stimulus-present trials where neurons are highly depolarized (in which case the stimulus is not relevant for the yes response) or from trials where the depolarization is not enough to reach the decision criterion, but the added effect of the stimulus suffices to obtain the correct response.

Decisions are choices made under uncertain conditions (9, 11, 14, 29, 31, 32). Tasks in which sources of uncertainty can be controlled provide excellent conditions to unveil the internal signals involved in decision-making processes. Noise correlations in cortical networks can be quite small (19, 20) and the observation of appreciable modulations in the covariation of pairs of neurons can be a signature of the presence of common internal signals. Our results could be pointing to a role of Bayesian inference in the cortical network where the internal signal reflects the animal's belief about the state of the world (33, 34) caused by the uncertainty about the amplitude and application time of the stimulus. Future experimental and theoretical work could clarify the connection between purely internal cortical processing and types of uncertainty in the task.

Materials and Methods

Data for this analysis were obtained from two earlier studies (11, 12). Monkeys were handled in accordance with institutional standards of the National Institutes of Health and the Society for Neuroscience. Protocols approved by the Institutional Animal Care and Use Committee of the Instituto de Fisiología Celular.

Neuronal recordings were obtained with an array of seven independent, movable microelectrodes (2–3 MΩ) inserted in areas VPc, DPc, and MPc, bilaterally. A total of 355 neurons were included in the analysis, on the basis of their response to any of the different components of the task and the stability of the recordings. Trials were classified according to monkey's choice and stimulus amplitude in hits, false alarms, misses, and correct rejections. Neural recordings were used for computing the firing rate and correlation coeffcients if there were at least five trials of the corresponding condition.

Firing rate as a function of time was calculated using a 250-ms sliding window displaced every 50 ms. To combine sets of trials with different stimulus amplitudes, we subtracted from each trial the mean firing rate of the set of trials with equal amplitude and divided by its SD. Correlation coefficients as a function of time were calculated from the firing rates of each pair of simultaneously recorded neurons following

$$\mathrm{CC}(t_i) = \frac{\langle v_1(t_i)v_2(t_i)\rangle - \langle v_1(t_i)\rangle\langle v_2(t_i)\rangle}{\sqrt{\mathrm{var}(v_1(t_i))\,\mathrm{var}(v_2(t_i))}},$$

where $v_k(t_i)$ is the firing rate of a neuron k at window i. Confidence intervals were estimated using a bootstrap technique. In each window we generated 500 resamples of the firing rates of the pair of neurons with the same number of trials as the original one. Resamples were drawn from the same collection of trials from which the CC was calculated. From these resamples we obtained a distribution of correlation coefficients and the confidence interval was considered proportional to the variance of this distribution (significance level: 90%, two sided). The mean temporal profile of the correlation coefficient over all pairs was computed using a weighted average. For each window and for each pair, the weight of the correlation coefficient value was considered proportional to the inverse of its confidence interval.

The analysis of slow covariations was done, computing the distribution of E over the population of pairs of neurons. We defined E as

$$E = \frac{1}{N}\frac{\sum n_i^k n_j^k}{\left(\frac{1}{N}\sum_{k=1}^{N} n_i^k\right)\left(\frac{1}{N}\sum_{k=1}^{N} n_j^k\right)} - 1,$$

where n_i^k and n_j^k are the spike counts of neurons i and j in trial k, computed in a time window of length $T = 500$ ms and N is the number of trials. Following this definition, any deviation from $E = 0$ indicates a covariation of the spike counts larger than that expected for independent neurons. Because E is computed from spike counts in time windows of length T, values of E different from zero indicate covariations at timescales longer than T. The distribution of E over the population of pairs was calculated in two 500-ms-long periods of the task: "before stimulus onset" from $t = 2$ s to $t = 2.5$ s following KD and "end of delay period" from $t = 3$ s to $t = 3.5$ s from SO. For the first period trials were considered only if stimulus was presented after $t = 2.5$ s following KD. The histograms were computed using a bin size of 0.1 and normalized with the total number of pairs.

ACKNOWLEDGMENTS. Funding was provided by Spanish Ministerio de Ciencia e Innovacion (MICINN) Grant FIS-2009-09433 (to F.C. and N.P.), by an International Research Scholars Award from the Howard Hughes Medical Institute (to R.R.), and by grants from the Dirección General de Asuntos del Personal Académico de la Universidad Nacional Autónoma de México and the Consejo Nacional de Ciencia y Tecnología (to R.R. and V.d.L.).

1. Hanes DP, Schall JD (1996) Neural control of voluntary movement initiation. *Science* 274(5286):427–430.
2. Shadlen MN, Newsome WT (1996) Motion perception: Seeing and deciding. *Proc Natl Acad Sci USA* 93(2):628–633.
3. Romo R, Brody CD, Hernández A, Lemus L (1999) Neuronal correlates of parametric working memory in the prefrontal cortex. *Nature* 399(6735):470–473.
4. Kim JN, Shadlen MN (1999) Neural correlates of a decision in the dorsolateral prefrontal cortex of the macaque. *Nat Neurosci* 2(2):176–185.
5. Gold JI, Shadlen MN (2000) Representation of a perceptual decision in developing oculomotor commands. *Nature* 404(6776):390–394.
6. Salinas E, Hernández A, Zainos A, Romo R (2000) Periodicity and firing rate as candidate neural codes for the frequency of vibrotactile stimuli. *J Neurosci* 20(14): 5503–5515.
7. Romo R, Hernández A, Zainos A, Lemus L, Brody CD (2002) Neuronal correlates of decision-making in secondary somatosensory cortex. *Nat Neurosci* 5(11):1217–1225.
8. Hernández A, Zainos A, Romo R (2002) Temporal evolution of a decision-making process in medial premotor cortex. *Neuron* 33(6):959–972.
9. Cook EP, Maunsell JHR (2002) Dynamics of neuronal responses in macaque MT and VIP during motion detection. *Nat Neurosci* 5(10):985–994.
10. Romo R, Hernández A, Zainos A (2004) Neuronal correlates of a perceptual decision in ventral premotor cortex. *Neuron* 41(1):165–173.
11. de Lafuente V, Romo R (2005) Neuronal correlates of subjective sensory experience. *Nat Neurosci* 8(12):1698–1703.
12. de Lafuente V, Romo R (2006) Neural correlate of subjective sensory experience gradually builds up across cortical areas. *Proc Natl Acad Sci USA* 103(39): 14266–14271.
13. Hernández A, et al. (2010) Decoding a perceptual decision process across cortex. *Neuron* 66(2):300–314.
14. Shadlen MN, Newsome WT (2001) Neural basis of a perceptual decision in the parietal cortex (area LIP) of the rhesus monkey. *J Neurophysiol* 86(4):1916–1936.
15. Nienborg H, Cumming BG (2009) Decision-related activity in sensory neurons reflects more than a neuron's causal effect. *Nature* 459(7243):89–92.
16. Miller EK (2000) The prefrontal cortex and cognitive control. *Nat Rev Neurosci* 1(1): 59–65.
17. Averbeck BB, Lee D (2003) Neural noise and movement-related codes in the macaque supplementary motor area. *J Neurosci* 23(20):7630–7641.
18. Constantinidis C, Goldman-Rakic PS (2002) Correlated discharges among putative pyramidal neurons and interneurons in the primate prefrontal cortex. *J Neurophysiol* 88(6):3487–3497.
19. Renart A, et al. (2010) The asynchronous state in cortical circuits. *Science* 327(5965): 587–590.
20. Ecker AS, et al. (2010) Decorrelated neuronal firing in cortical microcircuits. *Science* 327(5965):584–587.

21. Doya K (2008) Modulators of decision making. *Nat Neurosci* 11(4):410–416.
22. de Lafuente V, Romo R (2011) Dopamine neurons code subjective sensory experience and uncertainty of perceptual decisions. *Proc Natl Acad Sci USA* 108(49): 19767–19771.
23. de Lafuente V, Romo R (2012) Dopaminergic activity coincides with stimulus detection by the frontal lobe. *Neuroscience* 218:181–184.
24. Aston-Jones G, Cohen JD (2005) An integrative theory of locus coeruleus-norepinephrine function: Adaptive gain and optimal performance. *Annu Rev Neurosci* 28: 403–450.
25. Yu AJ, Dayan P (2005) Uncertainty, neuromodulation, and attention. *Neuron* 46(4): 681–692.
26. Goldman-Rakic PS (1995) Cellular basis of working memory. *Neuron* 14(3):477–485.
27. Merten K, Nieder A (2012) Active encoding of decisions about stimulus absence in primate prefrontal cortex neurons. *Proc Natl Acad Sci USA* 109(16):6289–6294.
28. Romo R, Schultz W (1992) Role of primate basal ganglia and frontal cortex in the internal generation of movements. III. Neuronal activity in the supplementary motor area. *Exp Brain Res* 91(3):396–407.
29. Schall JD (2001) Neural basis of deciding, choosing and acting. *Nat Rev Neurosci* 2(1):33–42.
30. Tanji J (2001) Sequential organization of multiple movements: Involvement of cortical motor areas. *Annu Rev Neurosci* 24:631–651.
31. Platt ML, Glimcher PW (1999) Neural correlates of decision variables in parietal cortex. *Nature* 400(6741):233–238.
32. Sheinberg DL, Logothetis NK (1997) The role of temporal cortical areas in perceptual organization. *Proc Natl Acad Sci USA* 94(7):3408–3413.
33. Beck JM, et al. (2008) Probabilistic population codes for Bayesian decision making. *Neuron* 60(6):1142–1152.
34. Rao RP (2010) Decision making under uncertainty: A neural model based on partially observable markov decision processes. *Front Comput Neurosci* 4:146.

Supporting Information

Carnevale et al. 10.1073/pnas.1216799109

SI Text 1. Statistical Model

1.1. Description of the Model. We have implemented a statistical model to explore the effect of the internal signal during the stimulation period. The model consists of two populations of $N/2$ neurons, referred to as populations S and B (1). The activity of each neuron is described by its membrane potential, which is computed as a sum of three components,

$$V_i = \begin{cases} V_{0i}^S + V_s^S + V_{\text{int}}, & \text{if neuron } i \in S \\ V_{0i}^B + V_s^B - V_{\text{int}}, & \text{if neuron } i \in B. \end{cases} \quad [S1]$$

The first component, $V_{0i}^k (k = S, B)$, is a random number for each neuron drawn from a multivariate Gaussian distribution with mean μ_V^k, SD σ_V, and correlation coefficient ρ,

$$p(V_{01}, ..., V_{0N}) = \prod_{i,j=1}^{N} p_2\left(V_{0i}^k, V_{0j}^k\right), \quad [S2]$$

where $k = S, B$ and

$$p_2\left(V_{0i}^k, V_{0j}^k\right) = \frac{1}{2\pi\sigma_V^2\sqrt{1-\rho^2}} \exp\left(-\frac{\left(V_{0i}-\mu_V^k\right)^2 + \left(V_{0j}-\mu_V^k\right)^2 - 2\rho\left(V_{0i}-\mu_V^k\right)\left(V_{0j}-\mu_V^k\right)}{2\sigma_V^2(1-\rho^2)}\right). \quad [S3]$$

This component corresponds to the membrane potential of the neuron in the absence of any input besides noise. Its mean value μ_V^k is equal for all neurons in population k. Population B has a higher mean potential in the absence of inputs ($\mu_V^B > \mu_V^S$). The SD σ_V was taken equal to 6.4 mV for all neurons. The mean correlation coefficient ρ represents the effect of common recurrent inputs to pairs of neurons and induces spiking covariations.

The second term of Eq. **S1**, V_s^k, represents the membrane depolarization evoked by the stimulus. It is obtained as

$$V_s^k = g^k(R_{S1}(s) - R_{S1}(0)), \quad [S4]$$

where g^k is the synaptic efficiency of the connection from sensory areas to the population $k = S, B$ and $R_{S1}(s)$ is a Poisson-distributed random variable that represents the firing response of primary somatosensory neurons to a stimulus of amplitude s. The mean firing rates of S1 neurons were obtained from ref. 2 for the 10 stimulus amplitudes used in the experiment.

The third term in Eq. **S1** represents a common internal signal. The model assumes an internal signal that takes positive continuous fluctuating values, drawn from an exponential distribution of mean μ_{int},

$$p(V_{\text{int}}) = \frac{1}{\mu_{\text{int}}} e^{-\frac{V_{\text{int}}}{\mu_{\text{int}}}}. \quad [S5]$$

This signal depolarizes equally every neuron from population S and hyperpolarizes in the same amount every neuron from population B ($V_{\text{int}}^S = -V_{\text{int}}^B = V_{\text{int}}$).

The firing rate of neuron i is obtained from its membrane potential according to a sigmoidal activation function with parameters $r_{\min}$, $r_{\max}$, c, and V_{th},

$$r_i = \frac{r_{\max} - r_{\min}}{1 + e^{-c(V_i - V_{th})}} + r_{\min}. \quad [S6]$$

The decision variable is taken as the difference of the mean activities of the two populations. A positive difference corresponds to a "yes" decision and a negative one to a "no" decision. Therefore, an affirmative decision is made when

$$\langle r \rangle_S > \langle r \rangle_B, \quad [S7]$$

where $\langle ... \rangle_k$ represents the average over the neural population $k = S, B$.

The model is simulated for a large number of trials and these are classified as yes or no responses according to Eq. **S7**. Within yes trials, those with zero amplitude are labeled as false alarms and those with amplitudes different from zero are hits. Similarly within no trials, correct rejections are those with null amplitude and misses are those with finite stimulus amplitudes. Once the trials are classified, it is possible to compute the psychometric curve predicted by the decision model and the statistical properties of the neural activity in each condition.

SI Text 2. Analysis of the Model

2.1. Internal Signal and Frequency of Each Condition. We start the analysis of the model, considering the frequency of false-alarm trials. When there is no stimulus, Eq. **S1** reduces to

$$V_i = \begin{cases} V_{0i}^S + V_{\text{int}}, & \text{if neuron } i \in S \\ V_{0i}^B - V_{\text{int}}, & \text{if neuron } i \in B. \end{cases} \quad [S8]$$

Fig. S1 shows schematically the effect of the internal signal. In the absence of sensory inputs, population B is more depolarized than population S ($\mu_V^B > \mu_V^S$, black lines). The internal signal depolarizes neurons from population S and hyperpolarizes in the same amount neurons from population B (blue lines). Therefore, low values of the internal signal produce correct rejections (Fig. S1*A*) whereas high values of internal signal can make $\mu_V^S + V_{\text{int}} > \mu_V^B - V_{\text{int}}$ and lead to false-alarm trials (Fig. S1*B*).

The frequency of false-alarm trials p_{fa} is determined by the ratio between μ_{int} and $(\mu_V^B - \mu_V^S)/2$. Specifically, the probability of a false alarm is approximately equal to the probability that $V_{\text{int}} > (\mu_V^B - \mu_V^S)/2$ (Fig. S1*C*). Using the distribution of μ_{int}, Eq. **S5**, we have

$$p_{\text{fa}} = \exp\left(-\frac{\mu_V^B - \mu_V^S}{2\mu_{\text{int}}}\right) \quad [S9]$$

from where the mean of the internal signal, μ_{int}, can be evaluated once $\mu_V^B - \mu_V^S$ is known:

$$\mu_{\text{int}} = -\frac{\mu_V^B - \mu_V^S}{2\ln(p_{\text{fa}})}. \quad \textbf{[S10]}$$

The difference $\mu_V^B - \mu_V^S$ affects the mean correlation coefficient in correct-reject trials because it affects the distribution of V_{int} in this type of trials (Fig. S1*C* and also *SI Text 2*, section 2.2). Therefore, $\mu_V^B - \mu_V^S$ is chosen to reproduce the mean correlation coefficient in correct-reject trials.

In stimulus-present trials, the effect of the internal signal is combined with the depolarization produced by the stimulus in each population, $V_{st}^k = g^k(R_{S1}(s) - R_{S1}(0))$, with $k = S, B$ (Fig. S2 *A* and *B*). From the experimental data (1) it is known that the stimulus depolarizes both populations and that this depolarization is higher in population *S*; that is, $g^s > g^B > 0$. As a result, the stimulus lowers the boundary value of the internal signal that separates the two conditions by $\frac{1}{2}(V_s^S - V_s^B) = \frac{1}{2}(g^S - g^B)\overline{R_{S1}}$, where $\overline{R_{S1}} = R_{S1}(s) - R_{S1}(0)$ (Fig. S2*C*). Therefore, in stimulus-present trials, the simulated behavioral response is a consequence of the combination of stimulus and internal signal. An affirmative response can be caused by a high-amplitude stimulus in the presence of a low internal signal or by a low-amplitude stimulus and a high internal signal.

Following an analysis similar to the one that led us to Eq. **S9**, the frequency of hit events in stimulus-present trials is

$$\begin{aligned} p_{\text{hit}}(s) &= \exp\left(-\frac{(\mu_V^B + V_{st}^B) - (\mu_V^S + V_{st}^S)}{2\mu_{\text{int}}}\right) \\ &= \exp\left(-\frac{\mu_V^B - \mu_V^S - (g^S - g^B)\overline{R_{S1}}}{2\mu_{\text{int}}}\right), \end{aligned} \quad \textbf{[S11]}$$

which is valid for each stimulus amplitude s. Summing over the N_s nonzero stimulus amplitudes, $(g^S - g^B)$ can be estimated as

$$g^S - g^B = \frac{2\mu_{\text{int}}}{\sum_s \overline{R_{S1}}}\left(\sum_s \ln(p_{\text{hit}}(s)) + \frac{\mu_V^B - \mu_V^S}{2\mu_{\text{int}}} N_s\right), \quad \textbf{[S12]}$$

where the value of $p_{\text{hit}}(s)$ for each amplitude is obtained from the experimental psychometric curve (2). The value of g^B affects the mean correlation coefficient in the miss condition (*SI Text 2*, section 2.2) so it is calibrated to reproduce the observed experimental value. Finally, the parameters of the activation function ($r_{\min}$, $r_{\max}$, c, and V_{th}) are adjusted to reproduce the values of mean firing rates in the experimental data.

2.2. Spike-Count Correlations. The model contains three sources of spike-count correlations: the correlation coefficient of V_{0i} (ρ), the common internal signal (V_{int}), and the common input from S1 (V_s).

In this study we considered the case in which the voltage correlations are very small; that is, $\rho = 0$. Therefore, during stimulus-absent trials, the only source of correlations in firing rates is the common internal signal. In general, the mean correlation coefficient in each condition will depend on the distribution of the internal signal in the same condition. When the internal signal follows an exponential distribution, it can be seen that the correlation coefficients in each condition grow with both the mean and the variance of distribution of internal signal conditioned to that type of trials. Because large values of internal signal lead to yes responses, the distribution of the internal signal conditioned to false-alarm trials will have high mean and variance. In consequence, noise correlations in false-alarm trials will be higher than in correct-reject trials. Moreover, the largest value of the internal signal that results in a correct rejection is approximately equal to half of the difference between μ_V^B and μ_V^S. Therefore, this difference is chosen to reproduce the observed mean correlation coefficient in correct-reject trials.

For the stimulus-present trials there is another contribution to noise correlations coming from the sensory stimulation. Because of this contribution, the mean correlation coefficient in miss trials is higher than in correct rejections even when the internal signal distribution conditioned to miss trials has smaller mean and variance. Noise correlations in stimulus-present trials are affected by the values of the synaptic efficiencies. In particular, an increase in the value of g^B produces an increase in the correlation coefficient of miss trials. Therefore, g^B is adjusted to reproduce the observed mean correlation coefficient of the miss condition.

Finally, we have assumed that the internal signal affects both populations. This assumption is not necessary and the model would also work if the signal affected only population *S*.

SI Text 3. Parameter Values

$N/2$	No. neurons per population	100
μ_V^S, μ_V^B	Mean value of the membrane potential in absence of inputs	−67.4 mV, −55 mV
σ_V	SDs of the membrane potential	6.4 mV
ρ	Correlation coefficient of the membrane potential	0.0
g^S, g^B	Synaptic efficiencies	1.7 mV/Hz, 0.2 mV/Hz
V_{th}	Threshold voltage of the activation function	−55 mV
c	Gain of the activation function	0.5
$r_{\max}$	Maximum rate of the activation function	55 Hz
$r_{\min}$	Minimum rate of the activation function	16 Hz

1. de Lafuente V, Romo R (2006) Neural correlate of subjective sensory experience gradually builds up across cortical areas. *Proc Natl Acad Sci USA* 103(39):14266–14271.

2. de Lafuente V, Romo R (2005) Neuronal correlates of subjective sensory experience. *Nat Neurosci* 8(12):1698–1703.

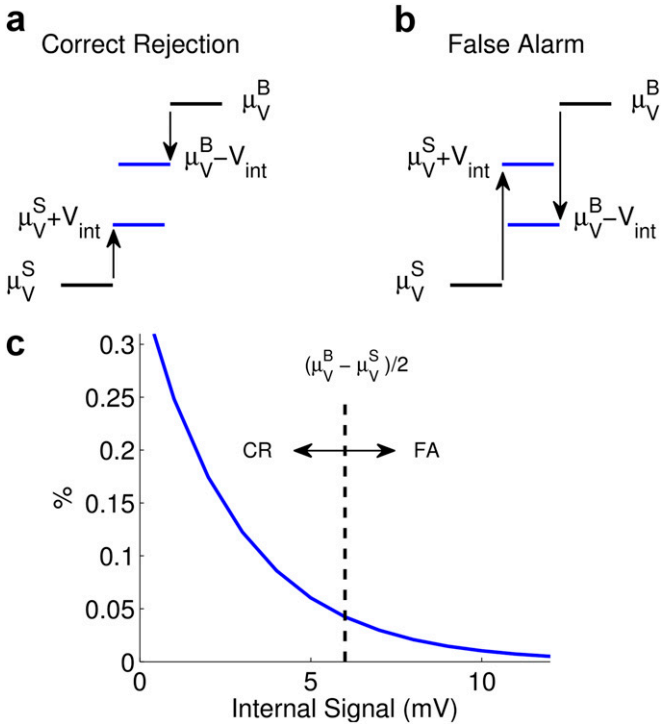

Fig. S1. Effect of the internal signal in stimulus-absent trials. The internal signal depolarizes neurons from population *S* and hyperpolarizes neurons from population *B* (blue lines). (*A*) Low values of internal signal produce correct rejection trials. (*B*) High values of internal signal can make $\mu_V^B > \mu_V^S$ and lead to false-alarm trials. (*C*) Because the internal signal is exponentially distributed, false alarms are less frequent than correct rejections.

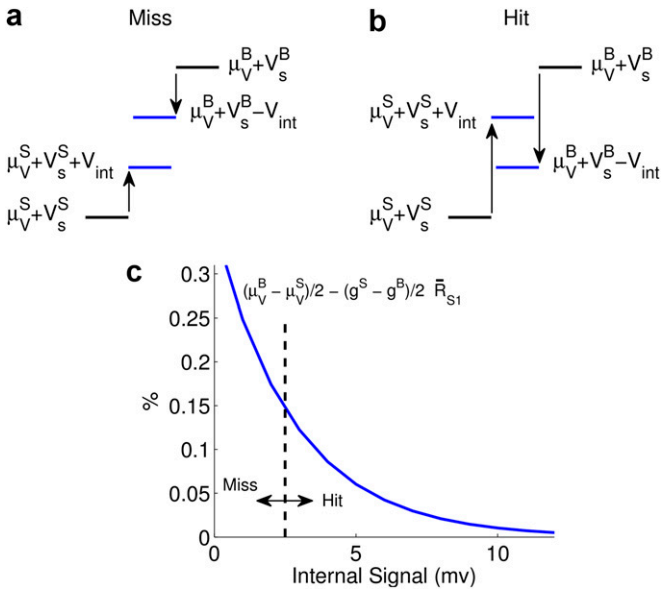

Fig. S2. Effect of the internal signal in stimulus-present trials. (*A* and *B*) In stimulus-present trials, the effect of internal signal is analogous to the stimulus-absent case (Fig. S1). (*C*) The depolarization due to the stimulus lowers the boundary value of the internal signal that separates the two conditions by a factor of $\frac{1}{2}(V_s^S - V_s^B) = \frac{1}{2}(g^S - g^B)\overline{R_{S1}}$.